Earth Surf. Dynam. Discuss., 1, 745–782, 2013
www.earth-surf-dynam-discuss.net/1/745/2013/
doi:10.5194/esurfd-1-745-2013

Earth Surface Dynamics
Discussions
Open Access

Morphological and sedimentological response of a mixed-energy barrier island tidal inlet to storm and fair-weather conditions

G. Herrling and C. Winter

MARUM – Center for Marine Environmental Sciences, University of Bremen, Germany

Received: 21 October 2013 – Accepted: 28 October 2013 – Published: 15 November 2013

Correspondence to: G. Herrling (gherrling@marum.de)

Published by Copernicus Publications on behalf of the European Geosciences Union.

Abstract

The environment of ebb-tidal deltas between barrier island systems is characterized by a complex morphology with ebb- and flood-dominated channels, shoals and swash bars connecting the ebb-tidal delta platform to the adjacent island. These morphological features reveal characteristic surface sediment grain-size distributions and are subject to a continuous adaptation to the prevailing hydrodynamic forces. The mixed-energy tidal inlet Otzumer Balje between the East Frisian barrier islands Langeoog and Spiekeroog in the southern North Sea has been chosen here as an exemplary study area for the identification of relevant hydrodynamic drivers of morphology and sedimentology. We compare the effect of high-energy wave-dominated storm conditions to mid-term tide-dominated fair-weather conditions on tidal inlet morphology and sedimentology with a process-based numerical model. A multi-fractional approach with five graduated grain-size fractions between 150 and 450 microns allows the simulation of corresponding surface sediment grain-size distributions. Net sediment fluxes for distinct conditions are identified: during storm conditions, bed load sediment transport is generally onshore directed on the shallower ebb-tidal delta shoals whereas fine-grained suspended sediment bypasses the tidal inlet by wave-driven currents. During fair-weather the sediment transport mainly focuses on the inlet throat and the marginal flood channels. We show how the observed sediment grain-size distribution and the morphological response at mixed-energy tidal inlets are the result of both, wave-dominant less frequent storm conditions and mid-term tide-dominant fair-weather conditions.

1 Introduction

Tidal inlets at barrier island systems connect the open sea with the back-barrier tidal basin. Typically, they feature an ebb-tidal delta seawards and a flood-tidal delta landwards of a deep inlet throat that is bordered by shallow sandy shoals and marginal flood channels (Hayes, 1979). Both, tidal flow constriction through the narrow inlet and wave

ESURFD

1, 745–782, 2013

energy dissipation on depth-limited ebb-tidal delta shoals account for local enhanced sediment transport and rapid morphological evolution.

Morphodynamics at mixed-energy tidal inlets are driven by the combined action of waves and tides and the relative contribution of these interacting forces largely determines the morphological and sedimentological response. Komar (1996), De Swart and Zimmermann (2009), Davis and FitzGerald (2010) and FitzGerald (2012) give recent and comprehensive reviews on morphodynamic processes at a large variety of tidal inlet systems. The early work of Hayes (1975, 1979) and a recent study applying process-based models (Nahon et al., 2012) classified mixed-energy inlet regimes on a range between tide-dominated and wave-dominated and suggested corresponding inlet geometries that are in equilibrium with the long-term energetic input from waves and/or tides. Sha and Van den Berg (1993) developed a descriptive model to explain ebb-tidal delta symmetry, i.e. the orientation of the seaward inlet channel with respect to shallow ebb-delta shoals, as a response to the relative direction of waves to the interplay of tidal currents alongshore and within the inlet. Very few studies at mixed-energy tidal inlets investigated the complex interaction of tide- and wave-driven processes and distinguished the contribution of each agent to residual sediment fluxes and morphological changes (e.g. Bertin et al., 2009; Elias and Hansen, 2013; Elias et al., 2006; Sha, 1989). Even less studies managed to relate observed distributions of surface sediment grain-sizes at tidal inlet systems to distinct physical drivers (e.g. Sha et al., 1990; van Lancker et al., 2004).

Recent studies have shown the applicability of process-based numerical models for sedimentological studies, e.g. to simulate surface sediment grain-size distributions in combination with morphological changes (Kwoll and Winter, 2011; Van der Wegen et al., 2010). This suggests the application of multi-grain size models to decipher the morphological and sedimentological effect of different hydrodynamic drivers, i.e. different model boundary conditions.

In this study we investigate the effect of tide- and wave-dominance on residual sediment pathways at a mixed-energy barrier island tidal inlet Otzumer Balje in the southern North Sea. It serves as example for a mixed-energy, slightly tide-dominant inlet regime with similar characteristics as e.g. described by Hayes (1979). This is achieved by simulating a storm surge event that represents a period of wave-dominance and fair-weather conditions with waves smaller than average representing tide-dominated conditions. Real-time data of tides, wind and waves are applied as forcing conditions for each model scenario, respectively, and are suggested to be sufficiently representative to study the morphological and sedimentological responses to low and high-energetic conditions. The following characteristics of tidal inlet systems are investigated:

1. Commonly it is understood that ebb-tidal delta erosion during episodic storm events counteracts the continuous replenishment of the ebb-tidal delta during tide-dominated fair-weather conditions (Swart and Zimmermann, 2009). We aim to show how this dynamic equilibrium behavior of either wave- or tide-dominated forcing conditions determines the sedimentology and morphology at an exemplarily mixed-energy tidal inlet and the adjacent foreshore. After a synthetic separation of tide- and wave-dominated forcing conditions, we will point out relevant morphodynamics and sediment pathways that are due to the interaction of the driving forces leading to e.g. elongated channel fill deposits at the margin of the tidal inlet throat.

2. Son et al. (2010) postulate a dominant circular sediment pathway at the eastern ebb-tidal delta platform of the here investigated tidal inlet Otzumer Balje. Sediments are thought to be recycled into the inlet throat without any evidence of sediment bypass to the downdrift beach. Other authors mention reversed sediment fluxes towards the inlet throat at Dutch barrier island tidal inlets but claim only minor significance with respect to the overall sediment dynamics (e.g.: Sha et al., 1990; Elias et al., 2006; Cheung et al., 2007). We evaluate the relevance of this recirculation cell at mixed-energy tidal inlets and identify the hydrodynamic drivers and interrelated mechanisms that induce these net circular sediment fluxes.

ESURFD
1, 745–782, 2013

2 Study area

The tidal inlet Otzumer Balje is located between the East Frisian barrier islands Langeoog and Spiekeroog in the southern North Sea. The back-barrier tidal basin represents a drainage channel system typical for the Wadden Sea. According to the classification of Hayes (1975, 1979), the study area is mesotidal with a mixed-energy to slightly tide-dominated regime. The tide is semidiurnal with a mean range of 2.8 m at Spiekeroog. The gorge in the inlet throat reaches maximal depths of circa 24 m below German datum (~ MSL) and a width of approximately 1 km. The residual flow in the inlet throat is ebb-dominant with maximal current velocities for neap- to spring-tides ranging from 0.5–1.0 $m\,s^{-1}$ and 0.8–1.6 $m\,s^{-1}$ for flood- and ebb-tide, respectively (Bartholomä et al., 2009).

Mean wind directions are from the westerly sector with mean velocities of about 7 $m\,s^{-1}$ observed at the offshore platform FINO1. Here, mean significant wave heights of 1.4 m and mean peak periods of 6.9 s have been measured (data of May 2004 to Juin 2006, Federal Maritime and Hydrographic Agency, BSH). Extreme storms from the north-westerly sector can generate surge water levels of up to 2.5 to 3.3 m above mean high water at the coast. During extreme event "Tilo" on 9 November 2007 significant wave heights of 10 m, maximal wave heights of 17 m and peak periods of up to 15 s were measured offshore at water depths of 30 m at the research platform FINO1 (Outzen et al., 2008). The combination of a tidal wave that travels from West to East and the dominant westerly wind and wave directions generate a longshore eastward-directed net sediment drift. FitzGerald (1984) estimated the net transport rate to about 270.000 $m^3\,yr^{-1}$ of sand.

The inlet consists of a variety of morphological features such as ebb- and flood-tidal deltas, inlet throat and marginal flood channels bordered by shoals and swash bars. The bed of the tidal inlet reveals different bed forms from ripples to dunes. In the inlet throat, Noormets et al. (2006) measured three-dimensional sand dunes with mean lengths of 7.5 m and mean heights of 0.35 m. Medium to coarse, poorly sorted sands

ESURFD
1, 745–782, 2013

are found in the inlet channel; the ebb-tidal delta body mainly consists of fine sand but is superimposed by swash bars of medium-sized sand (Son et al., 2010).

3 Methodology

3.1 Modeling system

The modeling system Delft3D (Deltares, 2011) has been applied to set-up and run high-resolution process-based morphodynamic models. The mathematical model solves the three-dimensional shallow water equations and continuity equation on a staggered model grid by use of an implicit finite-difference-scheme. The spectral wave model SWAN (Booij et al., 1999; Ris et al., 1999) is run in a stationary mode to simulate the wave propagation and deformation from the open sea to the shoreline. Bidirectional coupling of SWAN and the hydrodynamic module (Delft3D-FLOW) allows the exchange of relevant parameters on curvilinear model grids in time-intervals here assigned to 30 min. This coincides with the interval of available wave measurements applied as boundary conditions. Important wave effects are incorporated as wave-induced mass flux, turbulence and streaming in the wave boundary layer (Walstra et al., 2000). The interaction of wave forces (radiation stresses), tidal currents and the changing bed- and water levels is thus realized by a fully-coupled wave-current simulation. The here applied sediment transport formulation differentiates bed- and suspended load mechanisms (van Rijn, 2004). The model is used to identify sediment transport patterns between consecutive morphological states and to differentiate between instantaneous and residual suspended load and bed load directions and quantities. A detailed description of equations and processes implemented in the modeling system Delft3D is found in Lesser et al. (2004).

ESURFD
1, 745–782, 2013

3.2 Model nesting and boundary conditions

A hierarchical cascade of five model grids from the Continental Shelf to the East Frisian Barrier Islands with decreasing spatial dimensions and increasing numerical resolutions has been set-up to derive water levels and wave climate at the study area. In particular storm surge simulations require large model domains as coastal surge is generated by wind drag effects and atmospherical pressure gradients acting over long distances at open sea. The largest model with grid cell resolutions of 8000 m covers the Continental Shelf in the North Atlantic Ocean to the North Sea. Eight harmonic tidal constituents are applied to generate the astronomic tide at the sea boundaries of the Continental-Shelf-Model (Verboom et al., 1992). It embeds the Wadden-Sea-Model with average grid sizes of 1200 m covering the entire North Sea from the Dutch coast in the South to Denmark in the North. The Wadden-Sea-Model, in turn, generates water level time series at the seaward boundary of the smaller Ems-Elbe-Model with grid resolutions of approx. 200 m. The latter is additionally forced at the seaward boundary by wave data observed at the research platform FINO1 located 45 km offshore in water depths of 30 m. The next smaller model covers the East Frisian Barrier Islands from Juist to Wangerooge with model grid resolutions of 60–120 m and supplies wave- and water level boundary conditions to the most detailed Tidal-Inlet-Model covering only Langeoog and Spiekeroog islands. At the end of the model cascade, this 3-dimensional model with 10 sigma-layers over the vertical is dedicated to simulate the sediment dynamics at the tidal inlet Otzumer Balje and adjacent beaches (Fig. 1). It consists of 140 000 active grid cells with average grid resolutions of 60 m and up to 20 m in the breaker-zones, assumed to be sufficiently resolved for proper generation of wave-induced longshore currents.

3.3 Model bathymetry

Model bathymetries, i.e. depth schematizations for each particular model (Sect. 3.2), have been assembled by interpolating measured data of sea bottom elevations onto

ESURFD
1, 745–782, 2013

curvilinear model grids. Near coastal sub- and intertidal areas are covered by data of the years 2006, 2005 and 2001 based on conventional sounding methods (Federal Maritime and Hydrographic Agency, BSH). Elevations of inter- and supratidal barrier island beaches are partly covered by beach profiles of the year 2007 or high-resolution airborne LIDAR scans that are spatially limited and available for the years 2008, 2007 and 2005 (Coastal Research Station belonging to Lower Saxony Water Management, Coastal Defense and Nature Conservation Agency, NLWKN).

3.4 Meteorological forcing

Storms in the central part of the North Sea are associated with low-pressure systems. During the here reproduced extreme storm event "Tilo" between 5 and 10 November 2007 with peak surge levels on 9 November 2007, maximal wind velocities of $33\,\mathrm{m\,s^{-1}}$ and mean wind directions of North-North-West were recorded offshore (Outzen et al., 2008). Surge inducing wind stress and horizontal atmospheric pressure gradients acted over a large fetch from the Arctic Sea across the entire North Sea superimposed by high astronomical tide. The storm surge simulations are forced by meteorological model data of the German Weather Service (DWD). Wind and atmospheric pressure fields are available at 1 h intervals and spatial resolutions of 7 km and 2.8 km as for the COSMO-EU and COSMO-DE models, respectively.

The simulation representing fair-weather hydrodynamic conditions is forced by time series of wind data measured at the research platform FINO1 (Federal Maritime and Hydrographic Agency, BSH). Real-time data between 7 and 15 June 2007 are imposed to the wave and hydrodynamic simulations to account for a meteorological forcing with non-stationary wind velocities and directions. The mentioned period was selected based on visual comparison of generated wind roses due to the selected and a 2 yr data-set. Thus the selected data does not fulfill long-time statistical correctness, but the overall distribution of wind directions and intensity are similar to the long-time trend. Wind directions of the selected data series are from the westerly sector with

ESURFD
1, 745–782, 2013

a short intermittent period of easterly winds. The selected data is suggested to be sufficiently representative to account for typical low-energy wind- and wave conditions.

3.5 Bed layer model for multiple sediment fractions

A dynamic bed layer model is applied permitting the re-distribution of multiple sand fractions in relation to imposed bed shear stresses. Thus it enables the computation of spatial distributions of surface sediment grain-size fractions and to evaluate arithmetic mean grain-sizes in response to different hydrodynamic conditions. Each sand fraction depletes or increases in the bed cell according to erosion or deposition processes in the sediment transport formulation. A coefficient according to each mass-percent is applied in the transport equation to account for the availability of the mobilized sand fraction at a given bed-cell. Thus, sediment transport occurs if the critical shear stress for a certain grain-size fraction exceeds while its load is additionally controlled by the relative availability of each fraction. For details on the set-up and functioning of the bed layer model it is referred to Van der Wegen et al. (2010).

Within this study, model simulations were restricted to a limited number of five non-cohesive sand fractions with grain-sizes of 150, 200, 250, 350 and 450 µm because of computational expenses.

At first, preliminary simulations with fair-weather and storm forcing conditions, respectively, were initiated with a spatially uniform distribution of 20 mass-percent each (Fig. 8). Thus, the initial arithmetic mean grain-size equals 280 µm throughout the model domain. As the focus is on the sediment dynamics at the tidal inlet, a characteristic gradation of rather coarse sediment fractions between 150 and 450 µm was selected. According to this grain-size configuration, areas exposed to a low-energy wave impact such as the back-barrier tidal flats or the lower shoreface are hence not subject to significant morphological changes and thus grain-size sorting processes. Here, the initial arithmetic mean surface sediment grain-size of 280 µm did not change significantly during the simulations, although significantly finer sediments may occur in nature. This circumstance is tolerated here because back-barrier sediment dynamics and exchange processes between the back-barrier basin and the foreshore are not in the focus of this study. Back-barrier tidal flats contain high amount of fine sand and cohesive sediments and would require a different model set-up and grain-size configuration.

In a second step, to allow for a more realistic schematization of the surface sediment grain-size distribution at the area of interest, three model simulations with alternating hydrodynamic forcing conditions have been carried out. A simulation of 5 months being forced by fair-weather boundary conditions is followed by a storm surge simulation and another period of 5 months of fair-weather conditions. Sediment mass-fractions at the end of each model run are turned over to the consecutive simulation. The ultimate distribution of grain-sizes at the end of this sequence of simulations has been used for model validation purposes (Sect. 4.3). In addition, it serves as the initial distribution of grain-size mass-fractions for all other scenario model simulations where morphological changes and sediment fluxes are in the focus of the study (Figs. 4–7).

3.6 Morphological acceleration factor

A morphological scale factor is applied to account for the acceleration of bed-level changes during updates at each hydrodynamic time step (Roelfink, 2006). By use of this method which aims to economize computational run time, hydrodynamic time scales are adapted to much longer time scales of morphological evolution. Within this study, a morphological acceleration factor (Morfac) of 20 is applied during a simulation of 17 tidal cycles between neap and spring tide (7 to 15 June 2007) in order to account for morphological changes that occur during approximately 5 months of fair-weather conditions. For the storm surge simulation no morphological acceleration has been applied (Morfac = 1).

ESURFD
1, 745–782, 2013

4 Model validation

The applied model system Delft3D has been widely tested in morphodynamic modeling studies for various environments (e.g.: Lesser et al., 2004; Van der Wegen et al., 2010), yet is verified in comparably few morphological studies on non-idealized tidal inlets that take into account a real-world bathymetry (e.g.: Cayocca et al., 2001; Elias et al., 2006; Elias and Hansen, 2013). The validation of simulated morphodynamics by field observations is generally difficult as in-situ data is scarce and if at all, is only available for very limited areas. This does in particular apply to bathymetrical data measured just before and after a storm surge event in order to identify storm-induced bed evolution being crucial for model calibration and verification purposes. Available observations and published data of the studied tidal inlet and adjacent barrier islands beaches are summarized and compared to modeled hydrodynamics, sediment dynamics and surface sediment grain-size distributions in order to determine the validity of the modeling approach below. Model results are from the two most detailed model domains of the cascade of nested model grids (Sect. 3.2).

4.1 Hydrodynamics

Time series of simulated water levels are compared with observations at available tidal gauges within the study area. Figure 2 shows modeled vs. observed water level time series for the storm surge event at Spiekeroog tidal gauge. Generally, high water levels are well reproduced by the model; low water levels show discrepancies. The phase lag between modeled and measured water level time series is in the range of 10–20 min. Standard deviations for the water level amplitudes for the fair-weather and storm surge simulations are 12 cm and 19 cm at Spiekeroog and 14 cm and 22 cm at Langeoog, respectively.

During the storm surge event, wave observations are available at the back-barrier area of Langeoog and inside the surf-zone of Norderney. Maximal significant wave heights of 1.3 m were observed at the backbarrier of Langeoog (measurements of

ESURFD
1, 745–782, 2013

Helmholz Zentrum Geesthacht, HZG) that are overestimated by 17 % in the simulation. Significant wave heights of approximately 3.5 m that were measured in the surf-zone of Norderney at 9 November 2007 at 07:00 a.m. (Kaiser et al., 2008) are underestimated by 17 % in the simulation.

It shall be noted that no model calibration has been performed by bed roughness adaptation. The bed roughness has been set to a uniform, constant value over the model domain (Manning parameter 0.024); no locally adapted bottom roughness values have been set. In particular against this background, the hydrodynamic model results can thus be considered as sufficiently good.

4.2 Sediment dynamics and morphology

Time series measurements of suspended matter (SPM) concentrations observed at the tidal inlet Otzumer Balje during the storm surge peak on 9 November 2007 show hourly mean (maximal) values in the order of 35 (65) $\mathrm{mg\,L^{-1}}$ and 55 (95) $\mathrm{mg\,L^{-1}}$ for maximal flood- and ebb-tide currents, respectively, at 0.5 m below mean low water level (Badewien et al., 2009). The three finest sediment fractions incorporated in the model simulation (150, 200 and 250 µm) reveal hourly mean (maximal) SPM concentrations of 45 (70) $\mathrm{mg\,L^{-1}}$ during maximal flood-tide currents at 2 m below German datum at the location of the measuring pole. These SPM concentrations in the flood-directed inlet flow are due to nearshore wave-induced sand resuspensions and satisfactorily reproduced by the model. During ebb-tide, simulated maximal SPM concentrations of 2 $\mathrm{mg\,L^{-1}}$ are strongly underestimated with respect to measurements. This can be explained by the fact that fine sand (< 150 µm) and cohesive sediments that are typically flushed out of the backbarrier tidal flats during increased storm surge ebb-flows (Bartholomä et al., 2009; Cuneo and Flemming, 2000), are simply not incorporated in this model set-up. However, here, discrepancies are not relevant for this study, because the model is not applied to predict residual sediment rates between the foreshore and backbarrier basin.

Observations of morphological changes as a response to the storm surge event of 9 November 2007 are available for two cross-shore profiles at the foreshore of Langeoog

ESURFD
1, 745–782, 2013

island, both reaching from the beach until a distance of 3750 m from the shoreline into water depths of 14 m below German datum (data of observed profiles 37 and 38 at northshore Langeoog, Coastal Research Station, NLWKN, Kaiser et al., 2008). Measurements between August and October 2007 reveal relative changes of up to 1.0 to 1.5 m in the surf-zone and about 0.1 to 0.5 m in the foreshore. On the upper 600 m of the measured profiles, besides dune foot and upper beach erosion, morphological changes in the surf-zone show an offshore migration of a near shore-parallel bar. Changes within the foreshore (600–2000 m) are of erosional and depositional character and are related to the downdrift migration of two shore-oblique sand bars obliquely-oriented to the measured profiles. At 2000–3200 m from the shoreline, deposition in the order of 0.1–0.3 m is measured while on the last 500 m erosion of about 0.1 m occurs. The landward trough of the shore-face connected ridge at the end of the profiles tends to accumulate sand (3200–2700 m), whereas the adjacent slopes suffer from erosion. This data does not allow for model validation purposes, as the cross-shore bathymetrical data prior to the storm surge event (October 2007) deviates from the model bathymetry based on the year 2006. However, qualitative similarities of net morphological changes within the described morphological compartments are obvious, both, in magnitude as well as in alterations from net sedimentation to net erosion along the profile. Agreements between the modeled and measured morphological changes are generally better on the foreshore than on the much more dynamic beach.

4.3 Sedimentology

A mapping of surface sedimentology of the whole domain of interest is not available. However, Son et al. (2010) compiled surface sediment grain-size distributions in the Otzumer Balje tidal inlet from a grid of Shipek sediment grab samples at distances of approximately 280 m in the year 2005. Their data is re-interpolated here to allow for the comparison with modeled data. Modeled mean arithmetic surface sediment grain-sizes are due to re-distributions of five sand fractions between 150 and 450 µm for

ESURFD
1, 745–782, 2013

three alternating model runs with hydrodynamic forcings due to fair-weather conditions, storm conditions and again fair-weather conditions (Sect. 3.5).

The initial bathymetry of the detailed tidal inlet model is based on bathymetrical data of the years 2006/2007 and thus different from the inlet morphology of the sediment sampling campaign of 2005, here indicated by isolines based on available bathymetrical data of the years 2004/2005 (Fig. 3). The different morphological background explains the westerly bend of the channel through the ebb-tidal delta for the sampling state compared to a more straightened orientation in the model bathymetry.

Modeled and measured arithmetic mean surface sediment grain-size distributions show distinct similarities (Fig. 3). Surface sediments are coarsest at the inlet channel, the ebb-tidal delta and the eastern ebb-tidal delta shoal where swash bars migrate onshore. The central part of the ebb-tidal delta with medium to coarse sands is divided by a characteristic South–North oriented pattern of finer mean grain-sizes shown by both modeled and measured distributions. At the foreshore, modeled mean grain-sizes are generally coarser with respect to measurements.

The performance of the model to predict surface sediment grain-sizes increases for areas where the morphological changes are significant and thus sorting of sand fractions can take place. This may explain the discrepancies with respect to measured data at the foreshore. At the western ebb-delta shoals, on the other hand, distinct grain-size patterns of medium sand being predicted by the model cannot be validated by field data as the distance between sample positions (approx. 280 m) is too large in order to properly resolve these spatial patterns in surface sediment grain-sizes.

5 Results

Two model simulations are shown to compare the effect of an extreme storm surge event in the North Sea to a medium-term period (circa 5 months) of representative fair-weather conditions on morphodynamics and sedimentology at the tidal inlet Otzumer Balje between the barrier islands Langeoog and Spiekeroog.

ESURFD

1, 745–782, 2013

5.1 Fair-weather tide-dominated conditions

Residual total sediment transport fluxes during fair-weather conditions are largest in the vicinity of the tidal inlet and in particular in the inlet throat and the eastern marginal flood channel (Fig. 4a). The residual total load sediment fluxes are differentiated into residual bed load transports (Fig. 5a) and residual suspended load transports (Fig. 5b). Residual suspended load quantities are approximately 4 times larger than the residual bed load quantities but their residual directions are similar. North of the deepest location in the inlet throat, residual transport is ebb-dominant and directed towards the ebb-tidal delta while southwards it follows the inlet channel towards the flood-delta and the back-barrier basin.

Alongshore net sediment drift at the easterly end of the upcoast island Langeoog supplies bed- and suspended load towards the inlet throat of the tidal inlet. At the western ebb-tidal delta shoal, a residual sediment import to the inlet throat takes place over the shallow shoals whereas predominantly suspended sediment load is exported via ebb-channels located in between these shoals.

At the northern part of the eastern ebb-tidal delta shoal, minor residual bed and suspended load quantities are transported in a sharp bend from the center of the ebb-tidal delta to the eastern ebb-tidal delta shoal in a south-south-easterly direction. With increasing water depths landwards of the shoal, the sand is directed into a deeper, transverse tidal channel. Through this flood-dominant marginal tidal channel increased residual suspended and bed load quantities are transported in south-south-westerly direction back to the tidal inlet throat.

At the inlet widening towards the backbarrier tidal basin, the inlet throat is flood-dominated. Residual fluxes of predominantly suspended sediment point along the main channel towards the flood-tidal delta and adjacent tidal flats. At the northern margin of the main channel and alongside the western head of Spiekeroog, minor residual bed- and suspended load fluxes are opposite, thus ebb-directed via a bordering transport pathway. Between the easterly end of Langeoog and the flood-delta, a marginal tidal

ESURFD
1, 745–782, 2013

channel is also ebb-dominated and leads residual suspended and bed load fluxes out of the basin.

The mid-term fair-weather simulation reveals morphological and sedimentological changes at the tidal inlet and adjacent channels, at shore-parallel bars in the surf-zone and shore-oblique sand bars (Figs. 7a and 8a). Sediment dynamics at the foreshore are insignificant and net morphological changes are below 0.05 m (Fig. 7a). Sediments being eroded in the inlet throat and tributary channels are transported and deposited at the ebb-tidal delta and adjacent shoals. The most northern part of the ebb-tidal delta increases and protrudes offshore with net depositions exceeding 1.0 m at the ebb-delta lobe during the simulated period of 5 months.

The sediment distribution shows a coarsening of the mean surface sediment grain-size in the deep inlet throat, while the ebb-tidal delta lobe is fed by the entrained finer sand fractions (Fig. 8a). The depositional area at the ebb-tidal delta experiences a grading of sediment grain-sizes with mean grain-sizes as fine as 170 μm being deposited at the outermost ebb-tidal delta lobe where ebb-directed current velocities decrease due to increasing water depths.

Generally, it is noted that mean surface sediment grain-sizes in the inlet throat and marginal tidal channels are larger than 300 μm and up to 425 μm while finer sands tend to accumulate on elevated shoals and tidal flats.

Shore-oblique sand bars migrate eastwards in the same direction as the overall littoral sediment drift. Alike fluvial low energy bed forms, erosion takes place on the stoss-side and sedimentation on the lee-side (Fig. 7a). Their sedimentology reveals a gradient in mean surface sediment grain-sizes with medium (fine to medium) sands at the upper stoss-side and the crest (lee-side and trough) (Fig. 8a).

5.2 High-energy storm wave-dominated conditions

During the storm surge event, residual eastward directed total sediment fluxes are predicted to be largest at the barrier island foreshore and in particular directly off the ebb-tidal delta, while residual sediment load is insignificant in the tidal inlet throat (Fig. 4b).

The residual total load transport is differentiated in residual bed- and suspended load transport vectors (Fig. 6a and b). Disregarding the residual transport directions, the relative scaling of the vectors indicates that the net suspended load quantity is overall approximately one magnitude higher than the net bed load quantity. The residual bed load transport is south-south-eastward directed particularly at the eastern ebb-tidal delta shoal where it drives the migration of swash bars. The residual bed load transport direction agrees with the mean direction of wave propagation. Residual suspended sediment transport load is largest close to the ebb-tidal delta and in the extended surf-zone from the islands' beaches to the transition of upper to lower shoreface. Here, residual downdrift directed directions are due to wave-induced longshore currents that advect the entrained sand to the East.

During the storm surge event significant morphological and sedimentological changes occur over large areas of the barrier island foreshore and upper shoreface, but in particular at the tidal inlet and adjacent beaches (Figs. 7b and 8b). High-energetic waves refract and break on the depth-limited ebb-tidal delta shoals stirring large quantities of sediment. In the vicinity of the ebb-tidal delta, morphological changes along distinct linear patterns are predicted to be one meter and more during this storm event (Fig. 7b). Fine sand fractions of 150, 200 and 250 µm are transported as suspended load by the combined flow of tide-, wind- and wave-induced currents downdrift to the East. Mostly medium-sized sands with sand fractions of 250, 350 and 450 µm remain and thus increase the mean surface sediment grain-size of the ebb-tidal delta (Fig. 8b).

The morphology and sedimentology of the inlet throat and marginal flood channels is less affected as the driving wave energy is dissipated at the shallow ebb-tidal delta shoals. Grain-sizes insignificantly increase at the inlet gorge, whereas at the western margin of the inlet throat fine sands accumulate (Fig. 8b). Here, transport over the western ebb-tidal delta shoal directs finer sands south-south-eastwards to the western margin of the inlet throat causing a lateral shift of the inlet throat to the East (Fig. 7b).

At the eastern ebb-tidal delta shoal, alternating erosion and deposition patterns indicate a south-south-eastward migration of large swash-bars that are oriented almost

ESURFD
1, 745–782, 2013

parallel to the shore and thus deviate from shore-oblique sand bars (Fig. 7b). At the north-eastern edge of the ebb-tidal delta shoal, shore-oblique sand bars connecting the eastern ebb-tidal delta with the downdrift surf-zone migrate eastwards under storm conditions. A sediment distribution with coarser grain-sizes at the bedform crests with respect to the troughs is predicted for the swash-bars as well as for the shore-oblique sand bars (Fig. 8b).

At the shoreface, fine sand fractions are winnowed and eroded in the troughs between and at the landward slopes of shoreface-connected sand ridges being located in water depths of 15–20 m below German datum (Fig. 8b). Fine sand tends to accumulate on the crests and the seaward slopes of the shoreface-connected ridges. Thus the shoreface-connected ridges experience a positive morphological feedback and a downdrift migration (Fig. 7b).

6 Discussion

The main drivers determining the morphodynamic equilibrium of a mixed-energy tidal inlet system are commonly assumed to be waves which induce sediment stirring, transport and dispersal at the ebb-tidal delta and tidal-currents in the inlet (e.g.: De Swart and Zimmerman, 2009; FitzGerald et al., 2012). Mixed energy barrier island tidal inlets are morphologically highly dynamic environments where both drivers continuously interact. Numerical model scenario experiments allow the separation of processes and boundary conditions for in-depth system understanding. However, a potential model approach that either reduces the forcing to tides or waves alone would be misleading as the natural interaction at mixed-energy tidal inlets would be ignored. Instead, here, tide- and wave-dominated forcing conditions are represented by realistic fair-weather and storm scenarios, respectively, which allow the evaluation of the morphological and sedimentological responses to distinct hydrodynamic drivers by preserving the mixed-energy regime of the system at the same time.

ESURFD
1, 745–782, 2013

For typical mixed-energy tidal inlets, it is commonly assumed that ebb-tidal delta erosion during episodic storm events counteracts the continuous replenishment of the ebb-tidal delta lobe during tide-dominated fair-weather conditions (FitzGerald et al., 2012; Hayes, 1979). This study does reproduce and thus confirms this hypothesis: Model simulations of mid-term fair-weather conditions reveal that the morphological activity mainly focuses on the inlet throat. Eastward littoral drift along the foreshore beaches supplies fine sands into the inlet throat. In the deep inlet channel, bed shear stress due to tidal currents is strong enough to remove fine sands. As residual sediment fluxes in the seaward part of the inlet throat are ebb-directed the entrained fine sands mainly feed the ebb-tidal delta. During storm conditions, wave refraction and shoaling over steep bottom gradients focus wave energy towards the ebb-tidal delta lobe and its shallow shoals where energy dissipates due to wave breaking. Here, the fine sand deposited during fair weather periods is easily mobilised and transported eastwards by the ambient flow, dominated by alongshore velocity components induced by high-energy waves. These waves, approaching in an angle with respect to the shore, generate alongshore momentum flux that is greatest in the zone of breaking waves (Longuet-Higgins and Stewart, 1964).

Sediment grain-size sorting mechanisms and thus the spatial distribution of surface sediments are related to bed shear stress controlled by wave- and tide-induced flow: Residual distributions of surface sediment grain-sizes make clear that both, storm conditions with high-energy waves and fair-weather conditions where tidal currents dominate, contribute to the sedimentology of barrier island tidal inlets and foreshore. At the tidal inlet, for instance, we can generalize that winnowing of fine sand at the inlet throat and marginal channels is attributed to tidal forcing, whereas high-energy waves are the driver for sorting mechanisms at shallow shoals of the ebb-tidal delta (Fig. 8). Simulations have shown that only the combined scenario forcing, i.e. alternating fair-weather and storm simulations, result in a surface sediment grain-size distribution that is in fair agreement with sedimentological field observations at Otzumer Balje inlet (Fig. 3; Son et al., 2010). On its own, this gives evidence that the combination of both hydrodynamic

ESURFD

1, 745–782, 2013

forcing conditions is needed to determine the inlet sedimentological equilibrium. Furthermore, in light of the analogy of modeled and observed sedimentological patterns, this confirms the here applied model set-up to reliably simulate sediment dynamics in general and the evaluation of morphological and sedimentological features in response to representative boundary conditions in particular. The here applied model resolution and necessarily reduced multi-fractional approach proves the ability to reproduce gradients in grain-sizes on the spatial scale of morphological features equal and larger than swash bars and shore-oblique sand bars. Although smaller morphological features and bed forms such as ripples and dunes are not resolved in the model bathymetry, the here demonstrated modeling approach allows identifying distinct pathways of particular sediment grain-size fractions in response to wave-current interactions.

In the following, an example is given where simulated fluxes of particular sediment grain-sizes in combination with detailed information on three-dimensional hydrodynamics allow the identification of larger scale sorting mechanisms at the ebb-tidal delta lobe and the upper shoreface.

Surface sediment grain-size composition reveal simulated mass-fractions of up to 65 % and 35 %, respectively for sand fractions of 150 and 200 µm, which accumulate at the ebb-tidal delta terminal lobe during tide-dominated fair-weather conditions. Here, predicted mean grain-sizes are 170 µm and thus fairly agree with observations of 120 to 150 µm at "Otzumer Balje" (Son et al., 2010) and 120 to 180 µm at "Harle" (Hanisch, 2009), the tidal inlet to the East of Spiekeroog. The two finest sand fractions of 150 µm and 200 µm are obviously stirred by wave-action at the outer margin of the ebb-tidal delta but also bypass the inlet along the upper shoreface due to the storm-driven alongshore drift to the East. The finest fraction of 150 µm preferentially settles at areas of reduced energy off the downdrift Spiekeroog island within a shore-parallel band between the surf-zone and the sloping faces of the shoreface-connected ridges. Here, after the storm simulation, 20–30 % of the surface sediment is made up of this finest grain-size fraction of 150 µm. Antia (1995) observed an almost shore-parallel elongated pattern of accumulated fine sands with mass-fractions between 10–30 % for

ESURFD
1, 745–782, 2013

settling velocities of 1–1.5 cm s^{-1} which converts to grain sizes of 115–150 µm after Gibbs et al. (1971). Antia (1995) also describes this pattern to be extended between two bands of medium sands, respectively the surf-zone and the shoreface-connected ridges. The storm simulation reveals the physical process that explains this established deposit of fine sediments at the upper shoreface: Wave-induced currents counteract the opposing westerly-directed alongshore ebb-tidal currents in the expanded surf-zone. The ebb-tidal flow is restricted within this zone of wave-dominated longshore currents and shifted to deeper waters outside the surf-zone. This results in a band of reduced bottom shear at the interfacial boundary area of eastwards-directed wave-induced flow and westward-directed ebb-tidal flow. In this area settling of fine-grained sand is possible. Inside the surf-zone, wave-induced bottom currents are diverted off-shore in a shore-oblique angle due to the opposing ebb-currents. It is suggested that this offshore-directed undertow or downwelling (e.g. Niedoroda et al., 1984), supplies additional fine sand to the zone of reduced bottom shear; even if the latter process only is to some extent reproduced and rather underestimated by the model.

Besides these deposits of fine sand at the terminal lobe of the ebb-tidal delta and the shore-parallel band at the upper shoreface, additional characteristic spatial patterns that stand out by pronounced depositional processes within the surface sediment layer are identified. Particularly for storm conditions, the simulation reveals elongated channel fill deposits of fine-grained sand at the northern fringe of the marginal eastern flood-channel and even more pronounced at the westerly, sloping side of the inlet throat (Fig. 8b). The latter have been classified as channel margin linear bars (Hayes, 1979). Hubbart et al. (1979) have called this a "zone of equilibrium" where landward wave-induced flow over the marginal shoal platform is opposed and dominated by the ebb-directed tidal jet in the inlet throat. As described earlier, we identified several such zones of fine-grained deposits that evidently all have in common that tidal flow is partly or fully retarded and balanced by the opposing wave-induced momentum flux or vice-versa. This yields in a local reduction of bottom shear along the lateral interface of counteracting current fields and supports accumulation of fine-grained sediments. All

ESURFD
1, 745–782, 2013

Morphodynamic modelling of a mixed-energy tidal inlet

G. Herrling and C. Winter

other patterns at the tidal inlet and the foreshore region can be explained by erosional processes where fine sands are winnowed from surface sediments and thus medium to coarse sediment grain-sizes remain, e.g. the bottom of the tidal channels and the ebb-tidal delta shoals.

A simulation of tidal inlet morphology, sedimentology and sediment pathways calls for the identification of the communication and coupling of meso-scale hydro- and sediment dynamics between morphological units as e.g. the ebb-tidal delta shoals, the inlet channels and the adjacent barrier coast:

Hench and Luettich (2002) have shown in a numerical model study for an idealized and a natural inlet how momentum balances contribute to circulation processes by tidal forcing alone. The inlet jet induces a "dynamical wall effect" with momentum imbalances due to tidal phase lags resulting in transient, cross-inlet elevation differences and thus secondary circulation for different stages of the tide. With respect to the symmetrical geometry of their idealized inlet, the authors could show that the morphology of the natural inlet, i.e. particularly marginal tidal channels, plays an additional role in focusing the identified fluxes. In contrast to these tide-controlled circulation cells, FitzGerald et al. (1976) and Smith and FitzGerald (1994) describe "sediment gyres" downdrift of the inlet due to wave refraction and swash over the ebb-tidal delta shoal platform that drive swash bars in a net landward direction, while wave-induced set-up shoreward of the swash bars augment the inlet-directed currents in the marginal flood channel. Smith and FitzGerald (1994) conclude from sediment budgets due to assessed transport rates and morphological evolution analysis at the Essex River ebb-tidal delta system that the circulated sediment flux within the sediment gyres is estimated to be even larger than the amount that bypasses the inlet. Finley (1978) further adds by way of explanation refraction of moderate waves around the inlet ebb-tidal jet to be a process that contributes to ebb-tidal delta growth. The shoals are an efficient trap of littoral sediment drift that is reversed which otherwise would be carried alongshore.

These examples from literature show the importance of recirculation-cells for tidal inlet morphology and its budget in particular. Sediment dynamics involved are explained

ESURFD
1, 745–782, 2013

by physical processes which are either controlled by tides or waves. However, at mixed-energy tidal inlets, it is questionable which of the drivers contribute to the net circulation.

At the Otzumer Balje inlet residual sediment fluxes reveal a pronounced circulation-cell at the eastern ebb-tidal delta shoal. The circular pathway of particular grain-size fractions obviously is of importance for the overall sediment dynamics: During storm conditions, individual swash bar migration and wave-induced bed-load transport of medium sand point in landward direction over the eastern ebb-delta shoal platform. During fair-weather conditions, however, residual transport concentrates in the transverse, flood-dominated tidal channel southerly of the eastern shoal platform and leads towards south-westerly direction into the inlet throat. Once in the inlet throat, ebb-directed residual transport directs fine and medium sand to the ebb-tidal delta where the cycle restarts. Again, it is shown that solely the combination of wave-dominant storm and tide-dominant fair-weather conditions leads to net sediment fluxes describing a circular pathway easterly of the tidal inlet redirecting predominantly medium sand to the inlet throat.

The simulated sediment pathways confirm the conceptual model of Son et al. (2010), who already assumed a re-circulation cell over the eastern ebb-tidal delta shoal in this tidal inlet in which sediment is recycled towards the inlet throat. Their hypothesis was primarily derived from the orientation of sedimentary structures found in box- and vibro-cores. Sediment beds showed parallel lamination, which, according to the authors, originated from storm events being better preserved in the long-term than cross-laminated features generated during moderate conditions and that indicate dominant sediment pathways of medium-grained sand in a shoreward direction over the eastern ebb-delta shoal.

A separation in wave- and tide-dominated conditions allows the differentiation in residual sediment fluxes that contribute to the recirculation-cell. First, closed sediment circulation-cells are not recognized for storm conditions. Here, wave-induced bed load transport is onshore-directed over the shoal platform but no direct reversal to the inlet throat is evident. But during fair-weather conditions, a complete circulation-cell is apparent to a minor grade, however major transport is through the ebb-dominated inlet throat and the flood-dominated eastern marginal channel. Hence, we conclude that – at least for the here studied tidal inlet – a significant re-circulation of sand to the inlet is only possible as a combination of both fair-weather and storm conditions.

Another aspect addresses the mentioned sediment bypass at the Otzumer Balje inlet. Son et al. (2010) suggest that there is no evidence for fine sand bypassing the tidal inlet. If at all, bypassing would take place along the subtidal margin of the terminal lobe and be independent of processes acting on the ebb-tidal delta. However, no evidence was given to support this hypothesis, as no data was collected from regions seaward of the ebb-tidal delta. In disagreement to the hypothesis of Son et al. (2010), our simulations reveal sediment bypass to the downdrift beach and foreshore for both, moderate and extreme conditions. The magnitude of the bypass, seaward extent and the dominant grain-size are primarily controlled by wave-energy, i.e. wave-induced longshore currents, and consequently are increased for storm with respect to fair-weather conditions.

The question whether the net volume of sand that is re-circulated to the inlet throat is dominant over the bypassed quantity must be answered by future studies, as the simulated scenarios are either representative for tide- or wave-dominated conditions but non-representative for the long-term regime of this mixed-energy tidal inlet. Ongoing research aims to elucidate the sediment budget at the tidal inlet.

7 Conclusions

This study identifies residual sediment fluxes of particular grain-size fractions and related morphological and sedimentological responses of a mixed-energy tidal inlet system. We use a process-based numerical modeling system to differentiate the effects of either tide- or wave-dominant forcing. During storm conditions, the ebb-tidal delta loses sand through wave attack. For fair-weather conditions, the ebb tidal delta is replenished by ebb-directed residual sediment transports. The model simulations satisfactorily re-

ESURFD
1, 745–782, 2013

produce this well-known dynamic behavior. Sediment grain-size sorting mechanisms are likewise affected by the interacting tide- and wave-driven flow. We have shown that only a combined scenario forcing, i.e. alternating fair-weather and storm simulations, can result in a surface sediment grain-size distribution that is in agreement with measured grain-size distributions (Son et al., 2010). Medium-sized sand is either found at tidal inlet channels being exposed to tidal flow induced bottom shear or at the ebb-tidal delta shoals where winnowing of fine sand is a result of wave stirring. It is further shown that surface sediments at the barrier island foreshore and the inlet system in this setting can be explained by erosional and not depositional processes. Morphological patterns that are prone to depositional processes and accumulation of fine sand are identified to occur in zones of reduced bottom shear as a result of opposing tidal currents and waves.

The model confirms the significance of the re-circulation of sand via a semi-circular pathway at the eastern side of the ebb-tidal delta. Mainly medium-sized sands are redirected to the main inlet channel in a circular pattern over the eastern ebb-delta shoal and through the easterly marginal flood tidal channel taking into account the combination of residual sediment fluxes during both simulated scenarios. The model approach reveals that only the combination of wave-dominant storm and tide-dominant fair-weather conditions is able to achieve this net sediment re-circulation. In disagreement to earlier findings of Son et al. (2010), the model shows additional sediment bypass mainly by suspended sediment load to the downdrift foreshore and beach. The magnitude of the bypass, its seaward extend and the dominant grain-size fraction are primarily controlled by wave-energy, i.e. wave-induced longshore currents, and consequently are more increased for storm compared to fair-weather conditions.

The overall shape of the here studied exemplarily tidal inlet in the German Wadden Sea appears to be similar to typical textbook tidal inlets, e.g. described by Hayes (1979). Its geometry is characterized by a single ebb-dominated tidal inlet channel through the ebb-tidal delta and only a comparably slight asymmetric outline of the adjacent shoals to the downdrift. This allows the assumption that the here discussed

ESURFD
1, 745–782, 2013

processes and sediment pathway schemes are also applicable for many other mixed-energy tidal inlets at barrier island systems. This study thus reveals residual sediment transport pathways for tide- and wave-dominated conditions, respectively. It improves our understanding of complex sediment dynamics at mixed-energy tidal inlets as it identifies and qualitatively evaluates how the morphology and sedimentology responds to the contribution of distinct drivers that in nature are obscured by continuous interaction.

Acknowledgements. This study is associated to and funded by the research project WIMO (www.wimo-nordsee.de) being financed in equal parts by two ministries in Lower Saxony, the Ministry of Environment, Energy and Climate Protection and the Ministry of Science and Culture.

We gratefully acknowledge the authorities and institutes, namely the Federal Maritime and Hydrographic Agency (BSH) and the Coastal Research Station belonging to Lower Saxony Water Management, Coastal Defense and Nature Conservation Agency (FSK-NLWKN) for furnishing bathymetrical data, the Federal Ministry for Environment, Nature Conservation and Nuclear Safety (BMU) and the Project Management Jülich (PTJ) for providing measured data of waves and wind related to the research platform FINO1, the German Weather Service (DWD) for making meteorological model data available via the PAMORE database and the Senckenberg at Sea Wilhelmshaven (SaM) for furnishing in-situ data of surface sediment grain-size. Many thanks go to the great initiative of OpenEarth.nl (DELTARES) that is at the European forefront in disseminating high quality data, tools and models and in particular for making available the Dutch Continental Shelf Model (Verboom et al., 1992).

References

Antia, E. E.: Sedimentary Deposits Related to Inlet-Shoreface Storm Flow Interaction in the German Bight, Estuar. Coast. Shelf Sci., 40, 699–712, doi:10.1006/ecss.1995.0047, 1995.

Badewien, T. H., Zimmer, E., Bartholomä, A., and Reuter, R.: Towards continuous long-term measurements of Suspended Particulate Matter (SPM) in turbid coastal waters, Ocean Dynam., 59, 227–238, doi:10.1007/s10236-009-0183-8, 2009.

ESURFD

1, 745–782, 2013

Morphodynamic modelling of a mixed-energy tidal inlet

G. Herrling and C. Winter

Bartholomä, A., Kubicki, A., Badewien, T. H., and Flemming, B. W.: Suspended sediment transport in the German Wadden Sea – seasonal variations and extreme events, Ocean Dynam., 59, 213–225, doi:10.1007/s10236-009-0193-6, 2009.
Bertin, X., Fortunato, A. B., and Oliveira, A.: A modeling-based analysis of processes driving wave-dominated inlets, Cont. Shelf Res., 29, 819–834, doi:10.1016/j.csr.2008.12.019, 2009.
Booij, N., Ris, R. C., and Holthuijsen, L. H.: A third-generation wave model for coastal regions 1. Model description and validation, J. Geophys. Res., 104, 7649–7666, doi:10.1029/98JC02622, 1999.
Cayocca, F.: Long-term morphological modeling of a tidal inlet: the Arcachon Basin, France, Coast. Eng., 42, 115–142, doi:10.1016/S0378-3839(00)00053-3, 2001.
Cheung, K. F., Gerritsen, F., and Cleveringa, J.: Morphodynamics and sand bypassing at Ameland Inlet, the Netherlands, J. Coast. Res., 231, 106–118, doi:10.2112/04-0403.1, 2007.
Davis Jr., R. A. and FitzGerald, D. M. (Eds.): Beaches and Coasts, 4th Edn., Blackwell Publ., Malden, USA, 2010.
Deltares: User manual Delft-3D FLOW, available at: http://oss.deltares.nl/web/delft3d/manuals, 2011.
Elias, E. P. L., Cleveringa, J., Buijsman, M. C., Roelvink, J. a., and Stive, M. J. F.: Field and model data analysis of sand transport patterns in Texel Tidal inlet (the Netherlands), Coast. Eng., 53, 505–529, doi:10.1016/j.coastaleng.2005.11.006, 2006.
Elias, E. P. L. and Hansen, J. E.: Understanding processes controlling sediment transports at the mouth of a highly energetic inlet system (San Francisco Bay, CA), Mar. Geol., 345, 207–220, doi:10.1016/j.margeo.2012.07.003, 2013.
Finley, R. J.: Ebb-tidal delta morphology and sediment supply in relation to seasonal wave energy flux, North Inlet, South Carolina, J. Sediment. Res., 48, 227–238, doi:10.1306/212F743C-2B24-11D7-8648000102C1865D, 1978.
FitzGerald, D., Buynevich, I., and Hein, C.: Morphodynamics and facies architecture of tidal inlets and tidal deltas, in: Principles of Tidal Sedimentology SE – 12, edited by: Davis Jr., R. A. and Dalrymple, R. W., 301–333, Springer Netherlands, 2012.
FitzGerald, D. M.: Interactions between the ebb-tidal delta and landward shoreline; price inlet, South Carolina, J. Sediment. Res., 54, 1303–1318, doi:10.1306/212F85C6-2B24-11D7-8648000102C1865D, 1984.
FitzGerald, D. M., Nummedal, D., and Kana, T. W.: Sand circulation pattern at Price Inlet, South Carolina, in 15th Conference on Coastal Engineering, p. No. 15, Honolulu, Hawaii, 1976.

ESURFD
1, 745–782, 2013

Gibbs, R. J., Matthews, M. D., and Link, D. A.: The relationship between sphere size and settling velocity, J. Sediment. Res., 41, 7–18, doi:10.1306/74D721D0-2B21-11D7-8648000102C1865D, 1971.
Hanisch, J.: Sand transport in the tidal inlet between Wangerooge and Spiekeroog (W. Germany), Holocene Mar. Sediment. North Sea Basin Spec. Publ. 5 IAS, 35, 175, 2009.
Hansen, J. E., Elias, E., List, J. H., Erikson, L. H., and Barnard, P. L.: Tidally influenced alongshore circulation at an inlet-adjacent shoreline, Cont. Shelf Res., 56, 26–38, doi:10.1016/j.csr.2013.01.017, 2013.
Hayes, M. O.: Morphology of sand accumulation in estuaries: an introduction to the symposium, Estuar. Res., 2, 3–22, 1975.
Hayes, M. O.: Barrier island morphology as a function of tidal and wave regime, in Barrier islands, from the Gulf of St. Lawrence to the Gulf of Mexico, edited by: Leatherman, S., Academic Press, 1–27, New York., 1979.
Hayes, M. O.: General morphology and sediment patterns in tidal inlets, Sediment. Geol., 26, 139–156, doi:10.1016/0037-0738(80)90009-3, 1980.
Hench, J. L. and Luettich, R. A.: Transient Tidal Circulation and Momentum Balances at a Shallow Inlet, J. Phys. Oceanogr., 33, 913–932, doi:10.1175/1520-0485(2003)33<913:TTCAMB>2.0.CO;2, 2003.
Hubbard, D. K., Oertel, G., and Nummedal, D.: The role of waves and tidal currents in the development of tidal-inlet sedimentary structures and sand body geometry; examples from North Carolina, South Carolina, and Georgia, J. Sediment. Res., 49, 1073–1091, doi:10.1306/212F78B5-2B24-11D7-8648000102C1865D, 1979.
Kaiser, R., Niemeyer, H. D., Dirks, H., and Witting, M.: KFKI-Projekt DÜNEROS [03KIS063], doi:10.2314/GBV:611994755, 2008.
Komar, P. D.: Tidal-Inlet Processes and Morphology Related to the Transport of Sediments, J. Coast. Res., 23, 23–45, available at: http://www.jstor.org/stable/25736067, 1996.
Kwoll, E. and Winter, C.: Determination of the initial grain size distribution in a tidal inlet by means of numerical modelling, J. Coast. Res., SI, 2011.
Lesser, G. R., Roelvink, J. a., van Kester, J. a. T. M., and Stelling, G. S.: Development and validation of a three-dimensional morphological model, Coast. Eng., 51, 883–915, doi:10.1016/j.coastaleng.2004.07.014, 2004.
Longuet-Higgins, M. S. and Stewart, R. W.: Radiation stresses in water waves; a physical discussion with applications, Deep-Sea Res., 11, 529–562, 1964.

ESURFD
1, 745–782, 2013

Morphodynamic modelling of a mixed-energy tidal inlet

G. Herrling and C. Winter

Nahon, A., Bertin, X., Fortunato, A. B., and Oliveira, A.: Process-based 2DH morphodynamic modeling of tidal inlets: a comparison with empirical classifications and theories, Mar. Geol., 291–294, 1–11, doi:10.1016/j.margeo.2011.10.001, 2012.

Niedoroda, A. W., Swift, D. J. P., Hopkins, T. S., and Ma, C.-M.: Shoreface morphodynamics on wave-dominated coasts, Mar. Geol., 60, 331–354, doi:10.1016/0025-3227(84)90156-7, 1984.

Noormets, R., Ernstsen, V. B., Bartholomä, A., Flemming, B. W., and Hebbeln, D.: Implications of bedform dimensions for the prediction of local scour in tidal inlets: a case study from the southern North Sea, Geo-Mar. Lett., 26, 165–176, doi:10.1007/s00367-006-0029-z, 2006.

Outzen, O., Herklotz, K., Heinrich, H., and C., L.: Extreme waves at FINO 1 research platform caused by storm “Tilo” on 9 November 2007, DEWI Mag., 33, 17–23, 2008.

Ris, R. C., Holthuijsen, L. H., and Booij, N.: A third-generation wave model for coastal regions 2. Verification, J. Geophys. Res., 104, 7667–7681, doi:10.1029/1998JC900123, 1999.

Roelvink, J. A.: Coastal morphodynamic evolution techniques, Coast. Eng., 53, 277–287, doi:10.1016/j.coastaleng.2005.10.015, 2006.

Cuneo, P. S. and Flemming, B. W.: Quantifying concentration and flux of suspended particulate matter through a tidal inlet of the East Frisian Wadden Sea by acoustic doppler current profiling, in Muddy Coast Dynamics and Resource Management, Vol. 2, edited by: Flemming, B. W., Delafontaine, M. T., and Liebezeit, G., 39–52, Elsevier, doi:10.1016/S1568-2692(00)80005-4, 2000.

Sha, L..: Variation in ebb-delta morphologies along the West and East Frisian Islands, the Netherlands and Germany, Mar. Geol., 89, 11–28, doi:10.1016/0025-3227(89)90025-X, 1989.

Sha, L. P.: Surface sediments and sequence models in the ebb-tidal delta of Texel Inlet, Wadden Sea, the Netherlands, Sediment. Geol., 68, 125–141, doi:10.1016/0037-0738(90)90123-B, 1990.

Sha, L. P. and Van Den Berg, J. H.: Variation in Ebb-Tidal Delta Geometry along the Coast of the Netherlands and the German Bight, J. Coast. Res., 9, 730–746, available at: http://www.jstor.org/stable/4298126, 1993.

Smith, J. B. and FitzGerald, D. M.: Sediment Transport Patterns at the Essex River Inlet Ebb-Tidal Delta, Massachusetts, USA, J. Coast. Res., 10, 752–774, 1994.

Son, C. S., Flemming, B. W., and Bartholomä, A.: Evidence for sediment recirculation on an ebb-tidal delta of the East Frisian barrier-island system, southern North Sea, Geo-Mar. Lett., 31, 87–100, doi:10.1007/s00367-010-0217-8, 2010.

De Swart, H. E. and Zimmerman, J. T. F.: Morphodynamics of Tidal Inlet Systems, Annu. Rev. Fluid Mech., 41, 203–229, doi:10.1146/annurev.fluid.010908.165159, 2009.

Van Lancker, V., Lanckneus, J., Hearn, S., Hoekstra, P., Levoy, F., Miles, J., Moerkerke, G., Monfort, O., and Whitehouse, R.: Coastal and nearshore morphology, bedforms and sediment transport pathways at Teignmouth (UK), Cont. Shelf Res., 24, 1171–1202, doi:10.1016/j.csr.2004.03.003, 2004.

Van der Wegen, M., Dastgheib, A., Jaffe, B. E., and Roelvink, D.: Bed composition generation for morphodynamic modeling: case study of San Pablo Bay in California, USA, Ocean Dyn., 61, 173–186, doi:10.1007/s10236-010-0314-2, 2010.

Van Rijn, L. C., Walstra, D. J. R., and Van Ormondt, M.: Description of TRANSPOR2004 and implementation in Delft3D-ONLINE, Interim Rep. Prep. DG Rijkswaterstaat, Rijksinst. voor Kust en Zee. Delft Hydraul. Institute, Netherlands, 2004.

Verboom, G. K., de Ronde, J. G., and van Dijk, R. P.: A fine grid tidal flow and storm surge model of the North Sea, Cont. Shelf Res., 12, 213–233, doi:10.1016/0278-4343(92)90030-N, 1992.

Walstra, D. J. R., Roelvink, J. A., and Groeneweg, J.: Calculation of Wave-Driven Currents in a 3-D Mean Flow Model, in Coastal Engineering, 1050–1063, American Society of Civil Engineers, Reston, V A., 2000.

ESURFD

1, 745–782, 2013

Morphodynamic modelling of a mixed-energy tidal inlet

G. Herrling and C. Winter

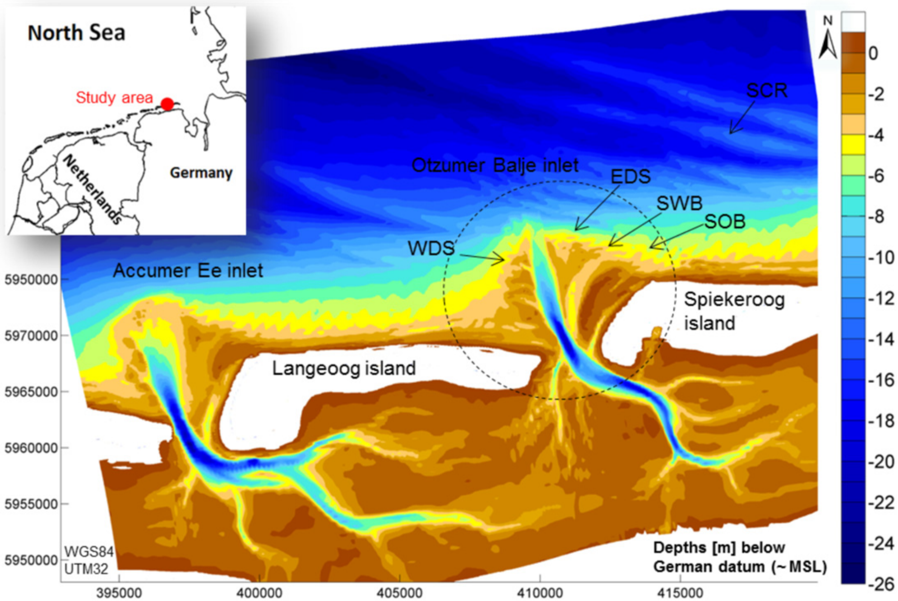

Fig. 1. East Frisian Barrier island system in the southern North Sea with the study area Otzumer Balje inlet between the islands Langeoog and Spiekeroog and nearshore morphological features such as the western/eastern ebb-tidal delta shoals (WDS/EDS), swash bars (SWB), shore-oblique sand bars (SOB) and shoreface-connected ridges (SCR).

ESURFD

1, 745–782, 2013

Morphodynamic modelling of a mixed-energy tidal inlet

G. Herrling and C. Winter

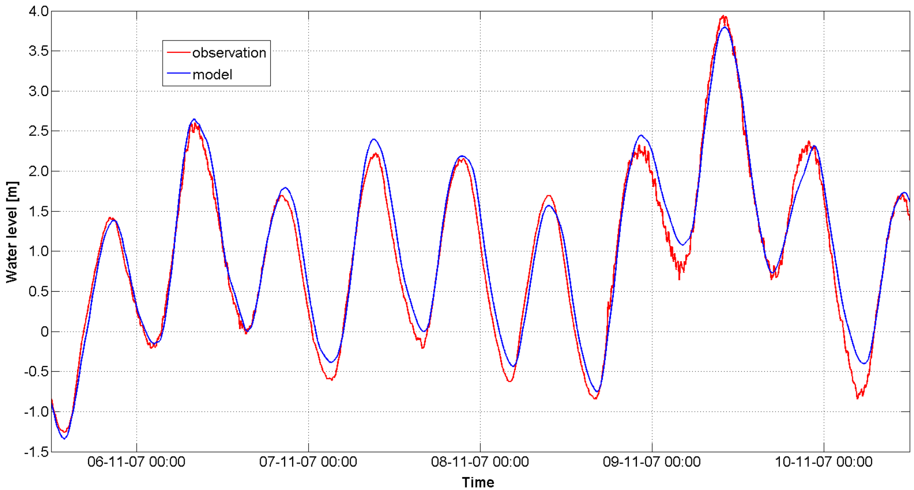

Fig. 2. Comparison of modeled (Delft3D-FLOW alone) and observed water level time series at water level gauge Spiekeroog for the storm event "Tilo" with peak surge levels on 9 November 2007.

ESURFD
1, 745–782, 2013

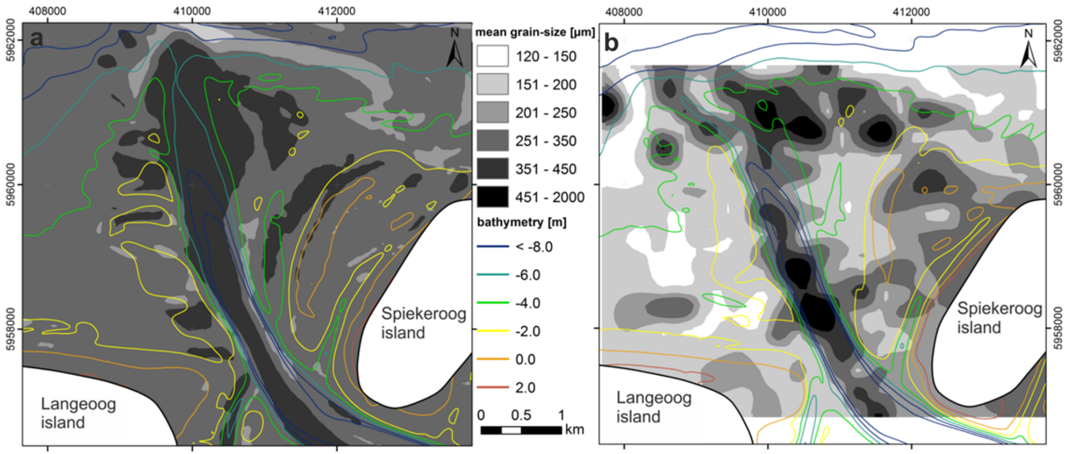

Fig. 3. Modeled **(a)** and measured **(b)** arithmetic mean surface sediment grain-size distributions at Otzumer Balje inlet between Langeoog and Spiekeroog islands; depths isolines based on bathymetrical data of 2006/2007 **(a)** and 2004/2005 **(b)**.

ESURFD

1, 745–782, 2013

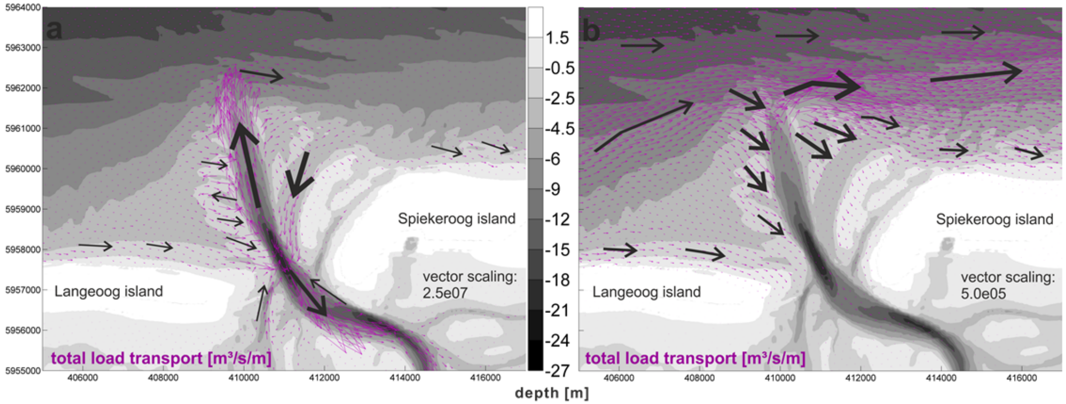

Fig. 4. Residual total load transport for fair-weather conditions **(a)** and storm conditions **(b)** and schematic main residual pathways indicated by black arrows.

ESURFD
1, 745–782, 2013

Morphodynamic modelling of a mixed-energy tidal inlet

G. Herrling and C. Winter

Title Page
Abstract Introduction
Conclusions References
Tables Figures
◀I ▶I
◀ ▶
Back Close
Full Screen / Esc
Printer-friendly Version
Interactive Discussion

ESURFD
1, 745–782, 2013

Morphodynamic modelling of a mixed-energy tidal inlet

G. Herrling and C. Winter

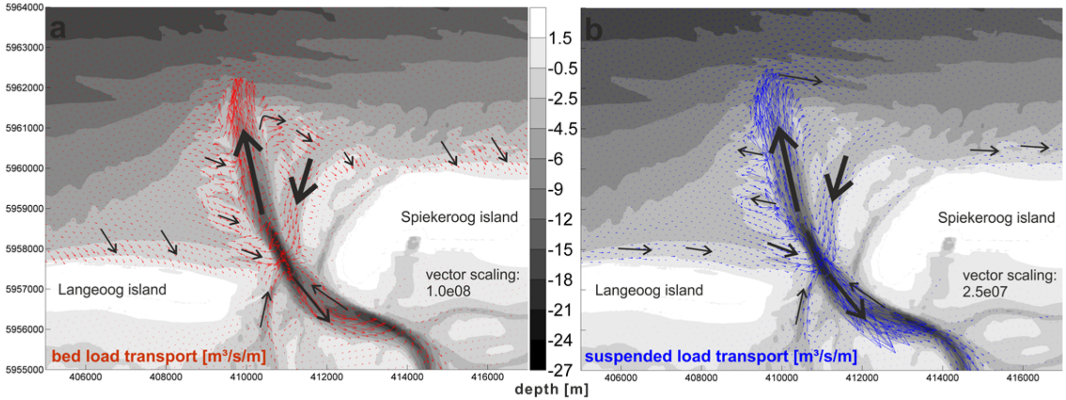

Fig. 5. Residual bed load **(a)** and residual suspended load **(b)** transport and schematic main residual pathways indicated by black arrows for mid-term fair-weather conditions; relative vector scaling indicates suspended load to be about 4 times larger than bed load transport.

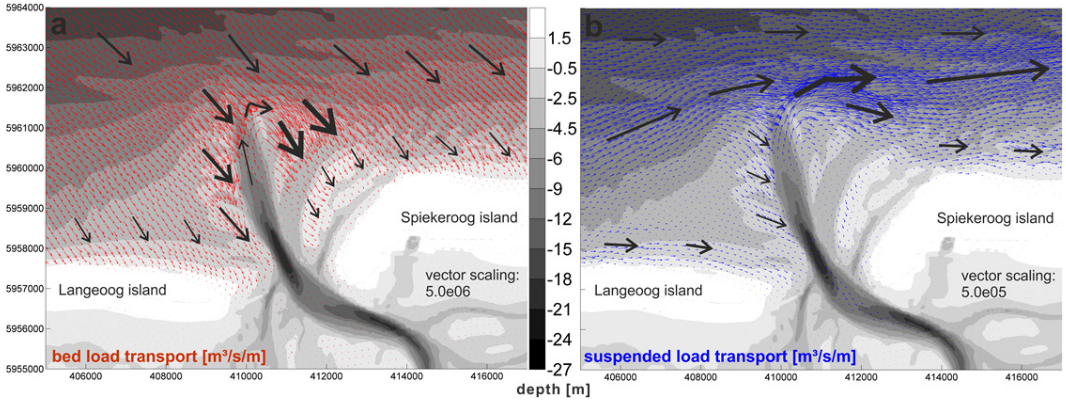

Fig. 6. Residual bed load **(a)** and residual suspended load **(b)** transport and schematic main residual pathways indicated by black arrows for high-energy storm conditions; relative vector scaling indicates suspended load to be about 10 times larger than bed load transport.

ESURFD
1, 745–782, 2013

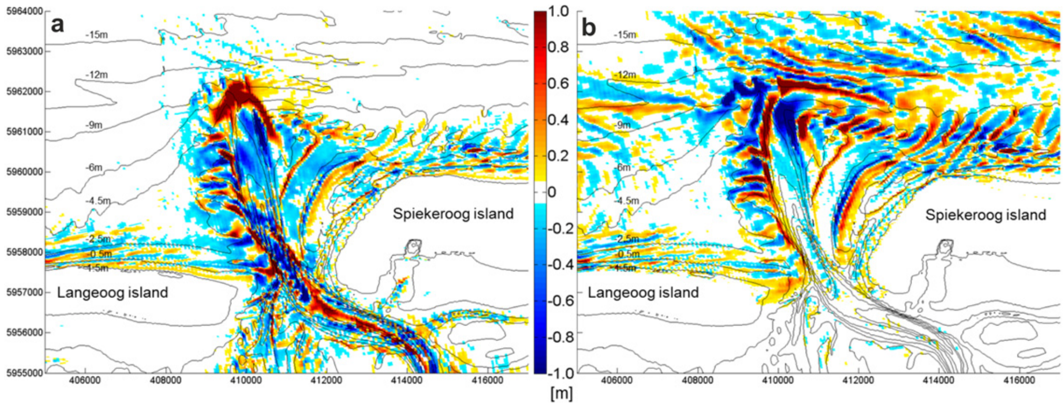

Fig. 7. Morphological changes, i.e. sedimentation (red) and erosion (blue) as a response to fair-weather **(a)** and storm **(b)** conditions; morphodynamic simulations have been initiated with already re-distributed surface sediment grain-size fractions (Fig. 3a).

ESURFD
1, 745–782, 2013

Morphodynamic modelling of a mixed-energy tidal inlet

G. Herrling and C. Winter

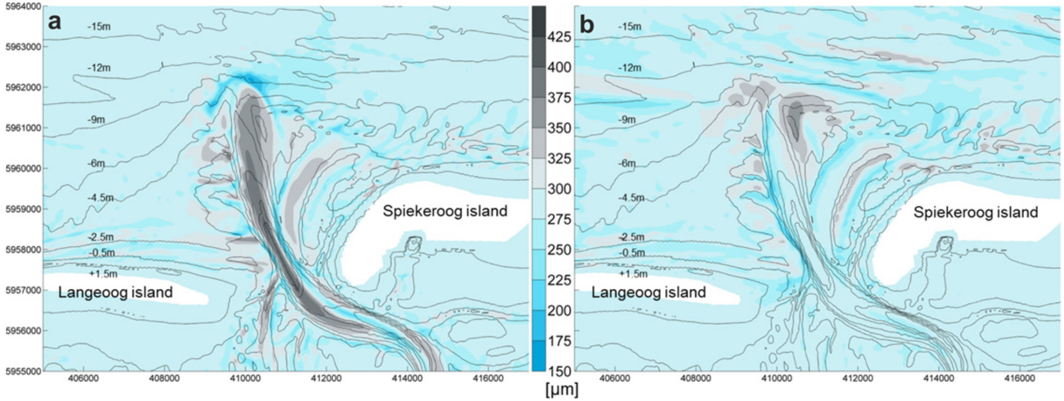

Fig. 8. Spatial distribution of arithmetic mean surface sediment grain-size as a response to fair-weather **(a)** and storm **(b)** conditions; simulations have been initiated with five equally distributed sand fractions of 150, 200, 250, 350 and 450 µm.

ESURFD
1, 745–782, 2013
Morphodynamic modelling of a mixed-energy tidal inlet
G. Herrling and C. Winter